



## Research Article

## Evaluating the Performance of a Humidification-Dehumidification Desalination System Integrated with Photovoltaic-Thermal Collectors

Sara Taheri<sup>a</sup>, Ahmadreza Faghih Khorasani<sup>a\*</sup>, Mohsen Mozafari Shamsi<sup>b</sup><sup>a</sup> Department of Mechanical Engineering, Yazd University, Yazd, Iran.<sup>b</sup> Department of Engineering, Meybod University, Meybod, Yazd, Iran.

## P A P E R I N F O

## Paper history:

Received: 06 October 2023

Revised: 18 December 2023

Accepted: 26 December 2023

## Keywords:

Desalination,  
Humidification-Dehumidification Technique,  
Collector,  
Photovoltaic-Thermal

## A B S T R A C T

Desalination stands out as a prominent method for obtaining fresh water from saltwater sources. The focus of this study revolves around a dehumidifier-dehumidifier system within a closed air-open water desalination framework, exploring two distinct modes: one without integration with solar collectors and the other incorporating solar collectors. Optimal conditions emerged with a fresh water circulation rate of 3 L/min and an incoming salt water flow rate of 1 L/min, resulting in a commendable maximum recovery ratio of 5.33%. Subsequently, in these optimal operating conditions, photovoltaic-thermal (PVT) panels were introduced to the desalination system, yielding insightful results. The output gain ratio (GOR), indicating the efficiency of converting heat to water evaporation, was 0.78 without connecting panels and 0.48 when panels were integrated. With panels connected, the desalination system achieved a peak fresh water production of 2.04 L/hr. Notably, the humidifier tower exhibited an impressive efficiency of 97%, while the dehumidifier tower operated at 40%. The solar collectors contributed significantly, meeting approximately 10% of the system's heating requirements and satisfying 7.3% of its electrical needs. The findings underscore the viability of integrating solar technology into desalination systems, showcasing not only increased fresh water output but also a noteworthy reduction in reliance on conventional energy sources. This innovative approach aligns with the global pursuit of sustainable and efficient water management solutions.

<https://doi.org/10.30501/jree.2024.417780.1696>

## 1. INTRODUCTION

In the first decades of the 21st century, the water crisis has become one of the most important crises in the world. Rapid industrial growth and population explosions around the world have intensified the demand for both fresh water for household and agricultural needs as well as the production of sufficient quantities of food (Lall et al., 2008). In addition, the problem of pollution of rivers and lakes due to industrial waste and sewage disposal has been added to other problems (Bose et al., 2017).

One way to overcome these problems is desalination (Abdullah et al., 2023; Garcia-Rodriguez, 2002; Kadhom, 2023). Desalination is the recently developed process of producing fresh water from impure or saline water. Different types of desalination methods have been proposed and developed by researchers that can be classified into membrane-based or heat-based methods (Fang, 2022; Srija et al., 2022; Xue et al., 2023). One of the heat-based methods of desalination is Humidification-Dehumidification (HDH), which has recently attracted researchers' attention extremely (Easa et al., 2024; Lai et al., 2023; Luberti & Capocelli, 2023; Srithar & Rajaseenivasan, 2017).

The basis of the operation of an (HDH) desalination system is the exchange of heat and mass transfer between the flow of humid saline water in different components of the system, to extract moisture from the air to establish saline airflow in the desalination system that requires an external source (Chehayeb et al., 2014). The thermal energy input to the HDH system can be supplied from solar energy. Photovoltaic-Thermal (PVT) type solar collectors are obtained from a combination of a conventional solar collector and a photovoltaic module (Herez et al., 2020). These collectors, while providing the necessary input heat to the HDH system, can provide some of the electrical power required to establish the flow of saline water and air in the system. In the PVT collector, the photovoltaic panel is cooled by the fluid, which prevents the drop in efficiency at high temperatures as well as preheating the inlet fluid to the humidifier tower. On the other hand, due to the combination of photovoltaic modules and solar collector in an integrated system, the optimal installation space can also be utilized (Hosseini & Sarhaddi, 2017).

Numerous theoretical and experimental studies have been performed to evaluate the performance of HDH systems and PVT collectors. Mortezapour et al. experimentally tested a solar humidifier-dehumidifier equipped with a PVT collector (Mortezapour et al., 2018). The evaluation of the proposed

\*Corresponding Author's Email: [faghih@yazd.ac.ir](mailto:faghih@yazd.ac.ir) (A. Faghih Khorasani)URL: [https://www.jree.ir/article\\_186794.html](https://www.jree.ir/article_186794.html)

system was conducted at three levels of both air velocity and saline water flow through the photovoltaic absorber plate. The results showed that the highest evaporator efficiency was about 88%, the highest condenser efficiency was about 61%, and the maximum fresh water produced was about 4.8 L/day. Arabi and Reddy numerically examined the effect of using various gases such as air, hydrogen, helium, neon, nitrogen, oxygen, argon, and carbon dioxide as the operating fluid on the performance of an HDH system (Arabi & Reddy, 2003). The results of their study show that in terms of heat transfer, hydrogen and helium gases, and in the case of mass transfer, argon gases and carbon dioxide have better performance compared to the air. Finally, they proposed carbon dioxide as a carrier gas in the HDH system. Narayan et al. conducted a comprehensive study of different types of solar desalination systems and showed that solar desalination based on the humidifier-dehumidifier process is the best technique of solar desalination due to its high energy efficiency (Narayan, Sharqawy, et al., 2010). Hermosillo et al. studied the performance of an HDH system experimentally and numerically (Hermosillo et al., 2012). The humidifier unit of their system consists of a cellulosic substrate through which saline water flows and provides a considerable level of evaporation, and the dehumidifier unit is a liquid-gas heat exchanger in which the wasted thermal energy is recovered from the condensation of water vapor in humid air to preheat the incoming saline water. The thermal energy required to initiate the system is supplied by an electric heater. They investigated the effect of some performance parameters to achieve better heat recovery in the system. In 2015, Hamed et al. theoretically and experimentally investigated an HDH system connected to a vacuum tube solar collector (Hamed et al., 2015). Their results showed that the use of saline water preheating by the solar collector before entering the humidifier unit can enhance the production of fresh water up to about 22 L/day and diminish energy consumption costs by about \$0.06 per liter of freshwater production. Elattar et al. studied the economics of a solar ventilation system connected to the HDH desalination system (Elattar et al., 2016). They examined freshwater production rate, cooling capacity, electricity consumption, economic index, and combined system performance coefficient under different designs and performance parameters. The results revealed that compared to conventional ventilation systems, the hybrid system proposed by them had a higher cooling capacity and coefficient of performance, as well as less electrical power consumption in hot and humid areas.

Much research has been performed on the types of humidifiers-dehumidifiers. In the present study, for the first time, the connection of PVT collectors to the HDH system has been utilized to preheat the saline water and also to provide the necessary electrical power to flow the airflow inside the combined system. Meanwhile, the use of moving packing distinguishes this device from that of previous studies (Elhenawy et al., 2023; Naeini et al., 2023). The present study is based on an experimental method, and a desalination system with known dimensional specifications was made and then tested. Parametric studies and the effect of different design and performance parameters on system efficiency are some of the items that have been studied.

## 2. MATERIALS AND METHODS/EXPERIMENTAL

Figure 1 depicts a schematic view of the system connected to PVT collectors and its components. The system's operation involves the initial entry of saline water with low temperature into the plate heat exchanger (element number 1 in Figure 1). By absorbing the heat of incoming fresh water, the saline water undergoes a slight preheating. Subsequently, the preheated saline water flows into the set of PVT collectors (element number 2 in Figure 1), where its temperature is further elevated before being directed to the heater (element number 3 in Figure 1). Controlled by the thermostat setting, the water temperature is raised to the desired level.

The heated saline water is then introduced into the humidifier tower through the nozzle (element number 4 in Figure 1), where it is sprayed onto the packings within the tower. Simultaneously, air is introduced from the tower's bottom by a fan (element number 5 in Figure 1). Within the humidifier tower, heat exchange and mass transfer occur, leading to an increase in the air temperature and humidity. The relative humidity of the airflow approaches saturation.

Continuing to the next stage, the humid airflow is propelled by the fan to the second part of the system, entering the dehumidification tower (element number 6 in Figure 1). This humid air effectively acts as a carrier, transporting water vapor from the humidifier tower to the dehumidifier tower. In the dehumidifier tower, fresh water is sprayed onto the packings at a low temperature. As the temperature decreases, some of the humidity is removed. The collected humidity, along with water sprayed on the packings, enters the fresh water tank (element number 7 in Figure 1). Notably, fresh water circulates continuously within the dehumidifier tower.

In order to analyze the equations governing this system, it is assumed that the system operates in steady-state and steady-flow conditions. Both parts of the humidifier tower and the dehumidifier towers are thermal insulators, and the air pressure is equal to the ambient pressure of Yazd city. The geographical and climatic conditions of the test site (Yazd) are given in Table 1.

**Table 1.** The geographical and climatic conditions of the test site (Yazd)

Longitude	latitude	Height above sea level	solar flux	average ambient temperature
31.8974° N	54.3569° E	1216 m	870W/m <sup>2</sup>	14°C

The equation of energy and mass conservation in the humidifier part is as follows:

$$\dot{m}_{sw} + \dot{m}_{da}\omega_{a,in} = \dot{m}_{br} + \dot{m}_{da}\omega_{a,t} \quad (1)$$

$$\dot{m}_{sw}h_{sw,t} + \dot{m}_{da}h_{a,in} = \dot{m}_{br}h_{br} + \dot{m}_{da}h_{a,t} \quad (2)$$

Also, the equation of energy and mass conservation in the dehumidifier part is as follows:

$$\dot{m}_{da}\omega_{a,t} = \dot{m}_{dw} + \dot{m}_{dw}\omega_{a,out} \quad (3)$$

$$\dot{m}_{fw}h_{fw,t} + \dot{m}_{da}h_{a,t} = \dot{m}_{fw}h_{fw,b} + \dot{m}_{da}h_{a,out} + \dot{m}_{dw}h_{dw} \quad (4)$$

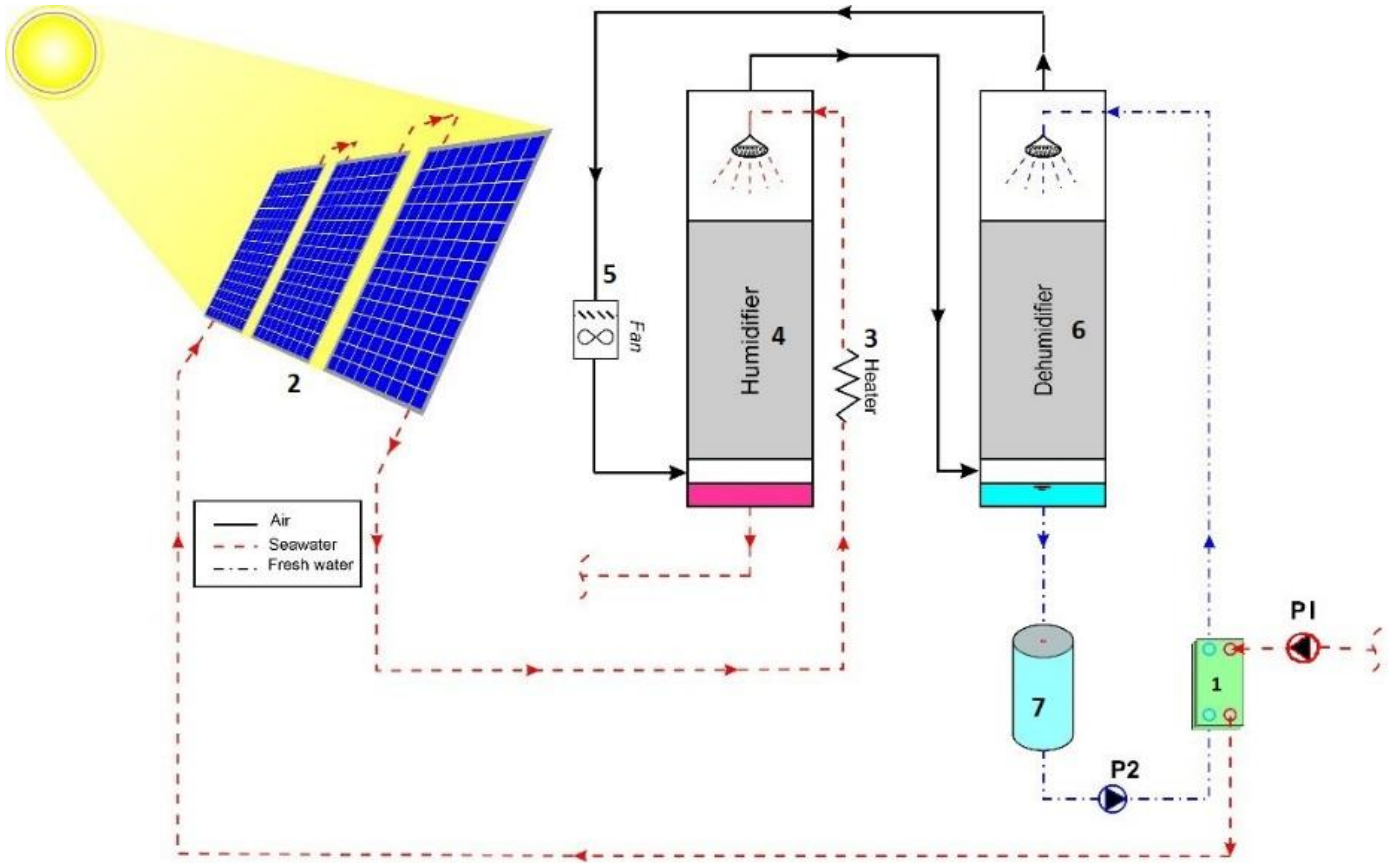


**Figure 1.** Schematic view of a water-desalination system with closed air cycle - open water with water preheating and photovoltaic panel

The heat energy required to heat the water can also be calculated as follows:

$$\dot{Q}_{in} = \dot{m}_{sw} c_{p,sw} (T_{sw,t} - T_{sw,b}) \quad (5)$$

$$\dot{Q}_{out} = \dot{m}_{fw} c_{p,fw} (T_{fw,b} - T_{fw,t}) \quad (6)$$

To evaluate the performance of the HDH desalination system, the output ratio (GOR) parameter is defined as the ratio of the latent heat of vaporization of the produced water to the total heat given to the system as follows (Dehghani et al., 2020):

$$GOR = \frac{\dot{m}_{dw} h_{fg}}{\dot{Q}_{in}} = \frac{\dot{m}_{dw} h_{fg}}{\dot{m}_{sw} c_{p,sw} (T_{sw,t} - T_{sw,b})} = RR \frac{h_{fg}}{c_{p,sw} \Delta T_{sw}} \quad (7)$$

The recovery ratio (RR) is the ratio of the mass flow rate of the produced water to the mass flow rate of the feed water and is defined as follows (Dehghani et al., 2019):

$$RR = \frac{\dot{m}_{dw}}{\dot{m}_{sw}} \times 100 \quad (\%) \quad (8)$$

To obtain the conditions in the humidifier and dehumidifier, the effectiveness of these parts should be evaluated. In fact, the effective parameter compares the transferred actual heat energy with the ideal heat energy from each flow and is defined as the change in the actual enthalpy rate to the maximum possible enthalpy rate change. The effective parameter is defined as follows (Narayan, Mistry, et al., 2010):

$$\varepsilon = \frac{\Delta \dot{H}}{\Delta \dot{H}_{max}} \quad (9)$$

The greatest possible change in enthalpy occurs when the device gives too much time and contact surface to the incoming currents to transfer mass and heat. The effectiveness of the humidifier and dehumidifier is determined by the following equations (Narayan, Mistry, et al., 2010):

$$\varepsilon_h = \max \left( \frac{\dot{H}_{a,t} - \dot{H}_{a,b}}{\dot{H}_{a,t} - \dot{H}_{a,b}^{ideal}}, \frac{\dot{H}_{sw,t} - \dot{H}_{br}}{\dot{H}_{sw,t} - \dot{H}_{br}^{ideal}} \right) \quad (10)$$

$$\varepsilon_d = \max \left( \frac{\dot{H}_{a,t} - \dot{H}_{a,b} + \dot{H}_{dw}}{\dot{H}_{a,t} - \dot{H}_{a,b}^{ideal} + \dot{H}_{dw}}, \frac{\dot{H}_{dw} - \dot{H}_{fw,t}}{\dot{H}_{dw} - \dot{H}_{fw,t}^{ideal}} \right) \quad (11)$$

In the above equations, air enthalpy is calculated using three parameters: air temperature, relative humidity, and ambient pressure in EES software. Meanwhile, the enthalpy of water is determined by two parameters: water temperature and ambient pressure. The ideal state of air enthalpy occurs when the temperature of the air leaving the humidifier matches the temperature of the saline water entering the tower, and its relative humidity reaches 100%. Furthermore, the enthalpy of water leaving each of the towers reaches an ideal state when the water temperature equals the temperature of the air entering the tower.

The heat efficiency of a plate heat exchanger is defined by the following equations:

$$Q_{heating} = \dot{m}_{sw} c_p \Delta T_{heating} \quad (12)$$

$$Q_{cooling} = \dot{m}_{fw} c_p \Delta T_{cooling} \quad (13)$$

$$\eta = \frac{Q_{heating}}{Q_{cooling}} \quad (14)$$

To calculate the efficiency of the water heater, the amount of electric consumption of the heater must be calculated. The

following equation is employed to calculate the efficiency of the heater (Dehghani et al., 2018):

$$\eta_{\text{Heater}} = \frac{Q}{W} = \frac{m \times C_p \times \Delta T}{V \times I} \quad (15)$$

A sample was prepared for the experimental study of the HDH desalination system. A moving packing was employed to enhance the heat transfer surface. The height of the packings in both the humidifier and dehumidifier towers is set at 1.25 m. This dimension was determined through experimental trials, comparing production levels at various packing heights, and accounting for potential constraints in system construction. Both the humidifier and dehumidifier towers utilize the same type of packing, and the shear section in both units is identical. In addition, a two-speed inter-channel fan with 120 W power, 2450 rpm motor speed, and an aeration volume of 720 m<sup>3</sup>/hr was utilized to generate airflow within the system. A damp channel, adjustable from 0° to 90°, was employed to regulate the airflow rate through the fan. Furthermore, the system incorporates pumps with a maximum head of 40 m and a flow rate of 40 L/min. By incorporating a bypass route, the flow rate of water passing through the packings can be adjusted. The saline water flow rate was varied within the range of 2-2.5

L/min, while the fresh water flow rate was adjusted between 0.5-3.5 L/min.

To monitor the system's conditions, humidity and air temperature were measured at two points: before entering the humidifier tower (point A) and before entering the dehumidifier tower (point B). Additionally, the air velocity in the duct was measured using a hot-air speedometer.

In this article, thermometers with an accuracy of  $\pm 1^\circ\text{C}$ , flowmeters with an accuracy of  $\pm 10^{-3}$  L/min, and a hot wire speedometer of  $\pm 0.01$  m/s were used. Additionally, two similar solar panels with dimensions of 25\*660\*1180 millimeters and a production power of 100 watts were used. Figure 2 shows the steps of making the system. Specifications of the used random splash packing (pall ring) are shown in Table 2.

After complete construction of the desalination system, optimization tests and performance evaluation of the device were initially performed in a roofed space without connection to PVT collectors, and then the device was transferred out of the workshop and connected to PVT collectors. Figure 3(a) shows a view of the device in the workshop space and Figure 3(b) shows a view of the device when connected to solar collectors.

**Table 2.** Specifications of used random splash packing (pall ring)

Packing Factor (m <sup>-1</sup> )	(%) void (m <sup>3</sup> /m <sup>3</sup> )	Surface area (m <sup>2</sup> /m <sup>3</sup> )	Num (pcs/m <sup>3</sup> )	Specification (D×H×δ)(mm)	Diameter (mm)
239	0.89	175	54000	1×25×25	25

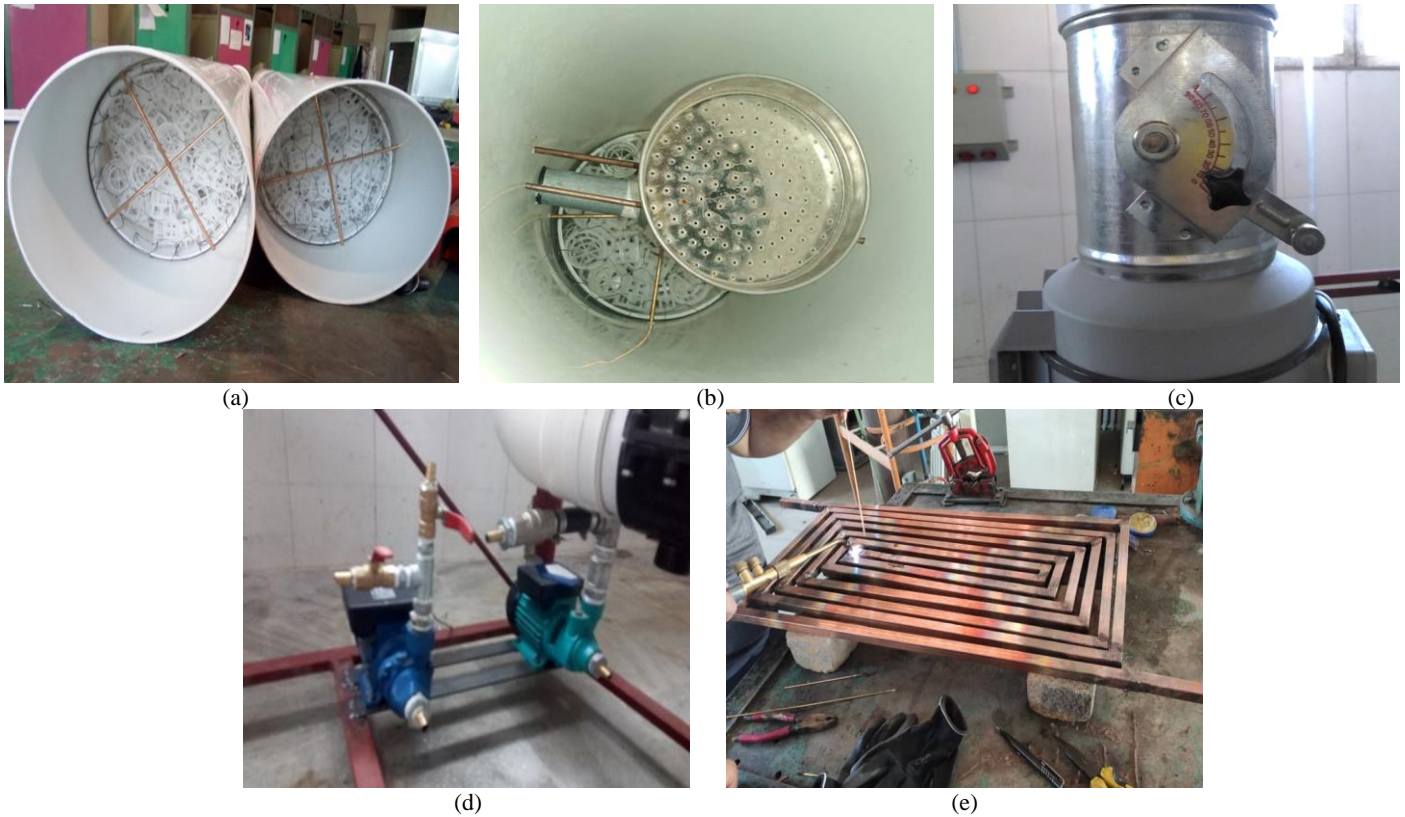


**Figure 2.** a) Interior view of humidifier and dehumidifier towers, b) Nozzle installation location in towers, c) Inter-channel and damp channel fan installed on the device, d) Water pumps for water circulation in the cycle, e) Construction of PVT collectors

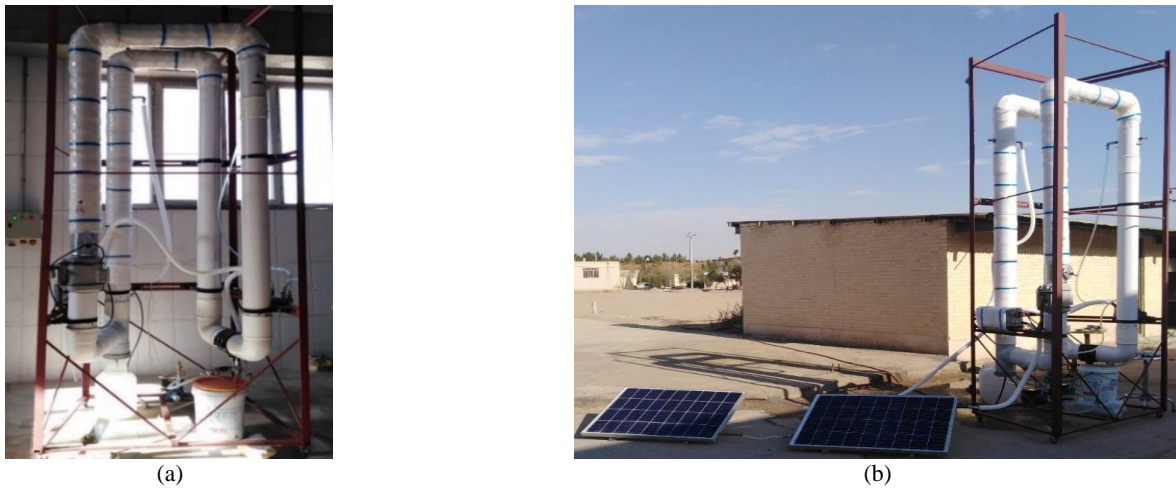


Figure 3. Desalination system (a) without and (b) with connection to PVT collectors

### 3. RESULTS AND DISCUSSION

To assess photovoltaic collectors, the experiment was conducted on a desalination system in two modes: with a collector and without a collector. Consequently, the results of the experiments were categorized into two groups: data pertaining to the unconnected state of PVT collectors and data related to the connected state of PVT collectors to the desalination system. In this research, the fresh water flow rate, salt water flow rate, and circulating air flow rate (adjusted with the help of damper adjustment) were regulated, and the remaining essential data were measured.

#### 3.1. Results in conditions without connection of PVT collectors to the desalination system

Firstly, to ascertain the appropriate air velocity in the channel, the fresh water flow, ranging from 0.5 to 3 L/min, and the saline water flow, ranging from 0.5 to 2 L/min, are fixed. At each specified time interval, the angle of the channel damper is adjusted, and the output is measured. Figure 4 illustrates the production rate at various flows and angles of the open channel. The optimal angle for the channel damper was found to be 30°. At this angle, the maximum fresh water production was achieved for different flows of incoming saline water and rotating fresh water. In this case, the average air velocity in the channel was 0.62 m/s.

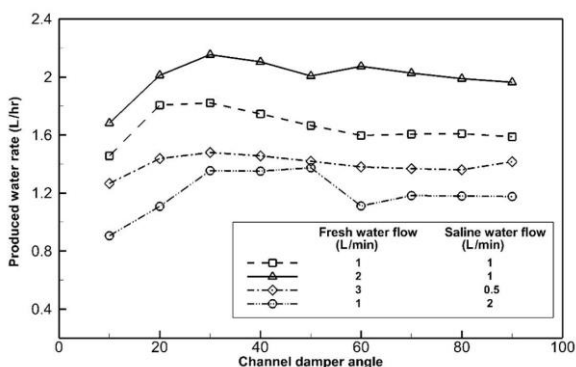


Figure 4. Diagram of water production rate at different angles of channel damper opening without connection to PVT solar collectors

In the next step, experiments were conducted to determine the most suitable saline water flow and fresh water flow. For this purpose, the damper angle was fixed at an optimal 30°, and

the saline water flow rate was set at 0.5 L/min. Subsequently, at specific time intervals, the fresh water flow rate was adjusted to 0.5, 1, 1.5, 2, 2.5, and 3 L/min, respectively, and the water production was measured at one-hour intervals.

In the subsequent steps, this experiment was replicated with saline water flow rates of 1, 1.5, and 2 L/min, and the results were meticulously recorded. The findings indicated that the highest volume of fresh water production was achieved when the saline water flow was 1 L/min, and the fresh water flow was 3 L/min. These test results are visually presented in Figure 5.

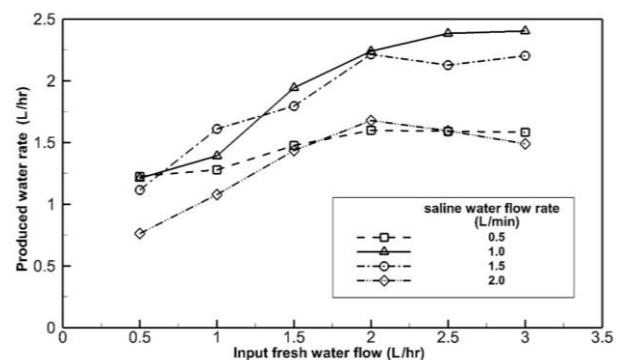


Figure 5. Diagram of water production rate at different discharges of saline water and fresh water, 30° angle of channel damper in case of no connection to PVT solar collectors

Also, utilizing the data from experimental assays, a diagram depicting the highest recovery ratio was constructed. The diagram presented in Figure 6 indicates that the lower the inlet saline flow rate, the higher the recovery ratio. At a flow rate of 0.5 L/min and a fresh water flow of 2 L/min, the highest recovery ratio was achieved, amounting to 5.33%. Similarly, the recovery ratio in the case of a saline water discharge of 1 L/min and a fresh water discharge of 3 L/min yielding the highest freshwater production in these discharges equaled 4.01%.

Figure 7 shows the gain output ratio (GOR) in different flows. GOR is an indicator for measuring heat recovery in the system. Equation (8) is used to calculate GOR. In Equation (8), the  $h_{fg}$  value is considered to be 2266 J/Kg. Since in the experiments performed, saline water was not available for use in the device, municipal water was used and the value of  $C_{p,sw}$  for all experiments was equal to 4.181 kJ/kg.K The recovery

ratio (RR) calculated in the previous step was placed in Equation (8) and the difference between the inlet saline temperature and the saline water temperature before entering the dehumidifier tower ( $\Delta T_{sw}$ ) was also obtained through measurements (Calculations are performed through EES software.).

The gain output ratio (GOR) is 0.78. Also, the highest GOR occurred at 1 L/min saline water flow and 3 L/min fresh water flow. GOR varies due to two parameters: recovery ratio (RR) and temperature difference ( $\Delta T_{sw}$ ). Increasing the fresh water flow rate at a constant saline flow rate increases the GOR. Increasing the temperature of the saline water entering the humidifier tower and decreasing the temperature of the fresh water entering the dehumidification tower also increases the GOR because these two factors increase the RR.

Furthermore, the efficiency of the humidifier tower under experimental conditions—specifically, with a saline water flow of 1 L/min and a fresh water flow of 3 L/min, without connection to PVT collectors—was calculated using Equations (10) and (11). The obtained value for the dehumidifier tower was 0.95, while for the humidifier tower, it was 0.4. Figure 8 compares the effectiveness of the dehumidifier tower and humidifier tower under different water discharge rates.

The efficiency of the heat exchanger in the state without a connection to the panel was 83.9% at a saline water flow of 1 L/min and a fresh water flow rate of 3 L/min. The incoming saline water experienced a temperature increase of 15.1 °C, while the fresh water was cooled by a rotating 6 °C. In these conditions, the heat energy extracted from the fresh water during rotation was 1255.3 W, and the heat energy transferred to the saline water was 1052.2 W.

To determine the efficiency of the water heater, we measured the current consumed by the heater, which was found to be 9 A. The heater efficiency under various saline and fresh water discharges is illustrated in Figure 9.

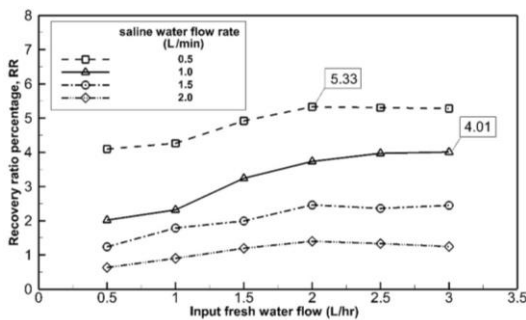


**Figure 6.** Recovery ratio at different discharges of saline water and fresh water, damper angle 30° without connection to PVT solar collectors

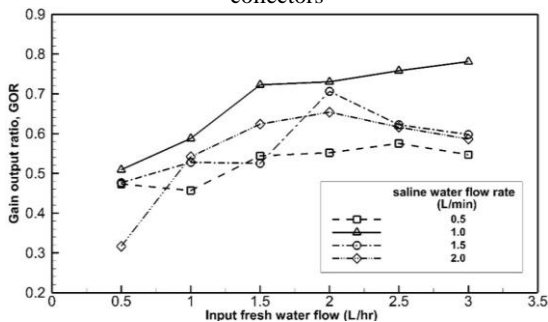


**Figure 7.** Diagram of the gain output ratio in different streams of saline and fresh water in the state without connection to PVT solar collectors

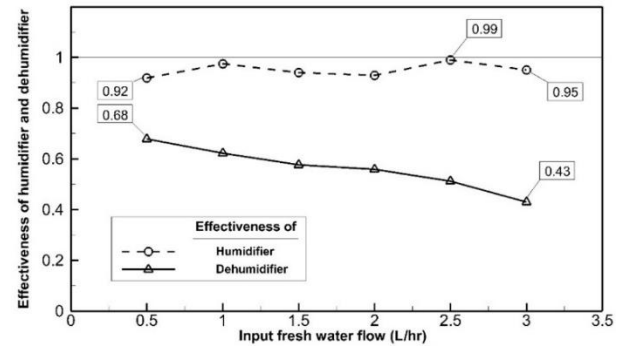


**Figure 8.** Diagram of the effectiveness of humidifier and dehumidifier towers in different saline and fresh water discharges without connection to PVT solar collectors

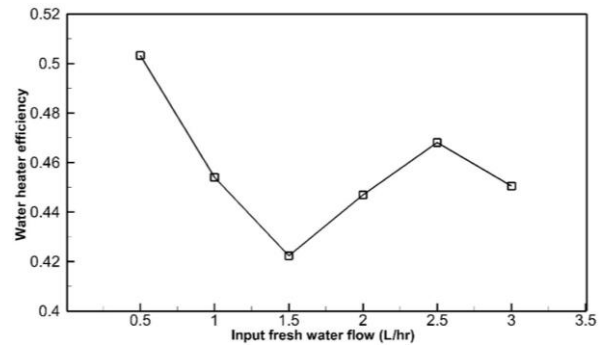


**Figure 9.** Water heater efficiency diagram without connection to PVT solar collectors

The efficiency of the heater at a saline water flow rate of 1 L/min and a fresh water flow rate of 3 L/min, without connection to PVT panels, was 45%. The amount of heat delivered to the saline water at this stage was 891.94 W. The results indicate that as the inflow of saline water increases, the efficiency of the heater decreases.

### 3.2. Results in connection of PVT collectors to the desalination system

After conducting experiments under conditions without connecting the desalination system to PVT collectors, we identified the optimal saline flow rate of 1 L/min, the optimal fresh water flow rate of 3 L/min, and the optimal damper angle of 30° for maximizing fresh water production. These optimal values were also applied when integrating PVT collectors into the desalination system to assess their impact on the results. For this purpose, the system was relocated from the workshop's enclosed space to an open area. After adjusting the necessary settings, PVT collectors were connected to the system. An experimental study was conducted on 11/18/2023 at this stage, with data collected three times per hour and subsequently averaged.

Figure 10 shows the production rate per hour. The maximum production was obtained between 11:30 and 12:30, which was equivalent to 2.04 kg/hr. Also, the production of the desalination system was 13.25 L/day. The average production was 1.89 kg/hr.

The graph of recovery ratio at different times of the day is shown in Figure 11. The maximum RR value is 11:30 - 12:30 and is equal to 3.4%. The average RR at a flow rate of 1 L/min of saline water and a flow rate of 3 L/min of fresh water and a 30-degree angle of the channel damper when connected to the panel is equal to 3.15%.

The graph depicting the output ratio at various times of the day is illustrated in Figure 12. The peak Gas-Oil Ratio (GOR)

value occurs between 10:30 and 11:30, reaching 0.51. The average GOR, observed at a flow rate of 1 L/min for saline water and a flow rate of 3 L/min for fresh water, with an open channel angle of 30°, is recorded as 0.48.

The effectiveness of the humidifier tower and dehumidifier tower is depicted in Figure 13. The humidifier tower outperformed the dehumidifier tower, with an average efficiency of 97% compared to the dehumidifier tower's average efficiency of 40%. When connected to the panel, the humidifier tower excelled because the solar collectors' heating elevated the water temperature. Additionally, the dehumidifier tower's performance was hindered by wind, resulting in poorer efficiency compared to the workshop space.

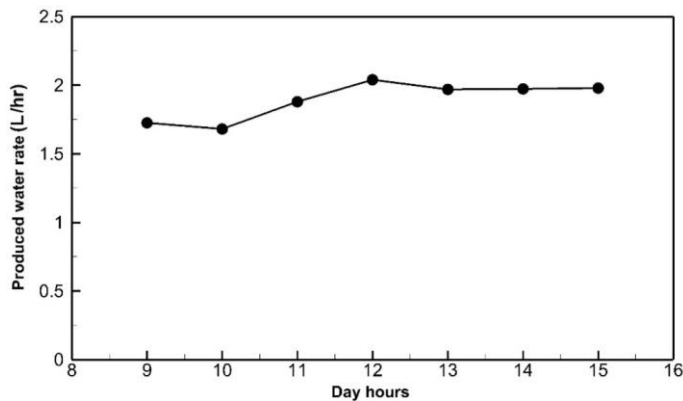


Figure 10. Diagram of water production rate when connected to PVT solar collectors

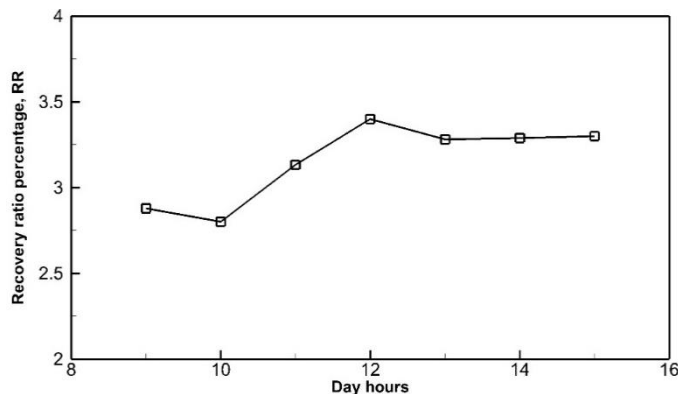


Figure 11. Percentage diagram of the system recovery ratio when connected to PVT solar collectors.

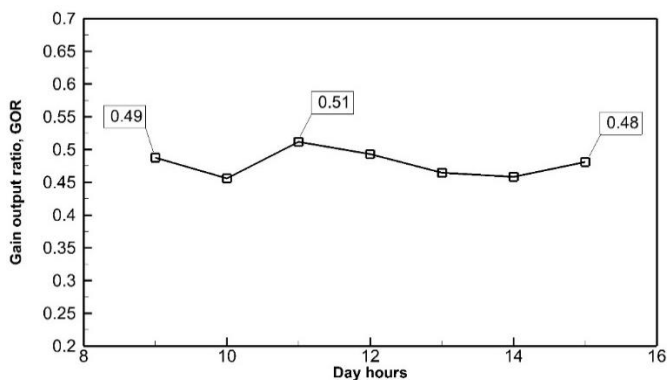


Figure 12. The graph of the output ratio obtained when connected to PVT solar collectors.

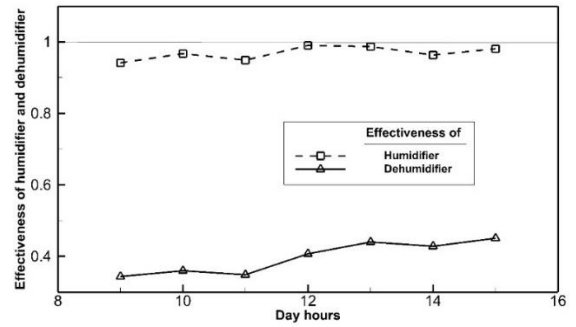


Figure 13. Effectiveness diagram of humidifier and dehumidifier towers when connected to PVT solar collectors.

As showed in Figure 14, the efficiency of the heat exchanger when connected to the panel was calculated to be 95.8% on average. In the preheating stage, an average of 821.6 W of heat energy is transferred to the water by the heat exchanger.

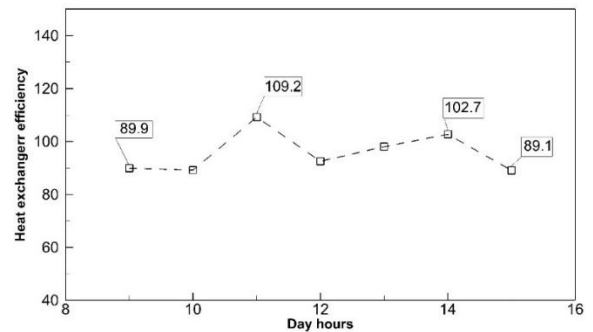


Figure 14. Heat exchanger efficiency diagram when connected to PVT solar collectors.

According to Equation (15), the efficiency of the heater per hour was calculated and its diagram is drawn in Figure 15. The average yield of the heater was 72%. During the heating phase by the heater, an average of 1433.49 W of heat energy is transferred to the water.

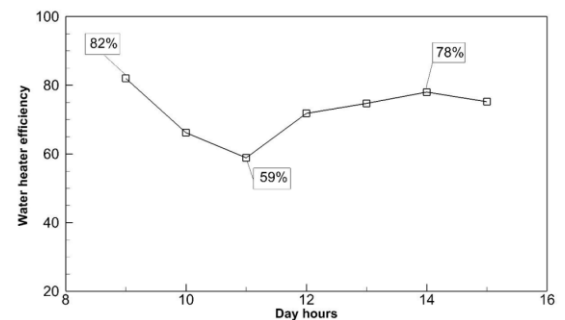


Figure 15. Efficiency diagram of water heater connected to PVT solar collectors

By passing water through the pipes behind the panel at a flow rate of 1 L/min, the water was preheated in the second stage, positively impacting the panel's performance. This is because reducing the working temperature of the photovoltaic cell improves its electrical efficiency (Sahay et al., 2015). The temperature differences observed at various times of the day are presented in Table 3. Additionally, using a voltage and amperage meter, the voltage reached 19.8 V, and the current reached 4.65 A, resulting in a calculated power of 92.07 W. This indicates a 14.87% increase in power produced by solar collectors.

As observed in Table 3, at 12 and 13 noon, the highest temperature difference occurred in saline water, with the greatest amount of heat energy extracted from the panel surface. On average, 225.97 W of heat energy is absorbed from the panel's surface and transferred to saline water.

**Table 3.** Temperature difference created by water passing through PVT panels

Data collection hours (hr)	Created temperature difference (°C)	The amount of taken heat from the panel surface and given to saline water (W)
9	0.8	58.07
10	3.1	218.34
11	3.7	255.51
12	4.1	283.38
13	4.1	283.38
14	3.8	267.12
15	3.1	216.07

### 3.3. Comparison of results in connection and non-connection conditions of PVT collectors to the desalination system

Comparable parameters, in two modes connected to panel and without panels, are presented in Table 4.

PVT collectors contribute 9.1% of the heat energy supplied to saline water. The power consumption of each system component is detailed in Table 5. In this system, 2530 W of electricity are consumed per hour. The heater stands as the largest consumer, while the fan is the smallest. Given that the output power of each panel is 92 W, and two PVT panels are employed, the system can generate 184 W of electricity per hour. The daily production of the panels amounts to 1288 W. This electricity can sufficiently power the fresh water fan and pump. Notably, the panels provide 7.3% of the required electrical power for the system.

**Table 4.** Comparison of test results in two modes connected to panel and without panel

Comparable parameters	Without panel	Connected to the pane
RR (-)	4.01	3.15
GOR (-)	0.78	0.48
Effectiveness of humidifier	95%	97%
Effectiveness of dehumidifier	43%	40%
Heater efficiency	45%	72%
Heat exchanger efficiency	83.9 %	95.8%
Heat exchanger efficiency rate Lit/h	2.4	2.04
The average amount of heat energy given to saline water in a heat exchanger (W)	1052.5	821.6
Average amount of heat energy given to saline water in the collector (W)	--	225.97
Average amount of heat energy given to saline water per heater (W)	891.94	1433.49
Average amount of heat energy given to saline water (W)	1944.14	2481.06

**Table 5.** Consumption of each system component

Components	current, (A)	Voltage, (V)	Power consumed (W)
Fan	0.2	220	44
Fresh water pump	0.6	220	132
Saline water pump	1.7	220	374
Heater	9	220	1980

### 4. Conclusion

In the present study, an HDH system connected to PVT collectors was fabricated to evaluate its performance. The effect of different performance and design parameters on the produced fresh water rate was investigated. The main results for the manufactured device are as follows:

- The optimal fresh water flow rate is 3 L/min and the optimal saline water flow rate is 1 L/min.
- The maximum recovery ratio of the desalination system was 5.33%.
- The recovery ratio of the desalination system, in case of non-connection of collectors, was 4.01%, and in case of connection of collectors, it was 3.15%.
- The gain output ratio in the two modes of disconnection and connection of collectors to the desalination system was 0.78 and 0.48, respectively.
- The maximum production in laboratory conditions was 2.4 L/hr. The peak production was achieved when the collectors were connected to the desalination system from 11:30 to 12:30, amounting to 2.04 L/hr. The performance of both heaters and heat exchangers improved when the collectors were connected to a desalination system. PVT collectors provided 9.1% of the heat energy to saline water and 7.3% of the electrical power required by the system, capable of supporting the fan and freshwater pump.
- The effectiveness of the humidifier improved in the outdoor desalination test, but in the case of the dehumidifier, the effectiveness decreased slightly.

### 5. ACKNOWLEDGEMENT

The authors would like to thank Yazd University for their support and providing construction workshops.

### NOMENCLATURE

#### English symbols

$C_p$	Specific heat capacity at constant pressure, $kJ/kg.K$
GOR	Gain output ratio (-)
$\dot{H}$	Enthalpy rate, $kW$
$h$	Enthalpy, $kJ/kg.K$
HDH	Humidifier – Dehumidifier
$I$	Electrical current, $A$
$\dot{m}$	Flow rate, $L/min$
PV	Photovoltaic collector
PVT	Photovoltaic-Thermal collector
$\dot{Q}$	Heat transfer rate, $kW$
RR	Recovery ratio (-)
$T$	Temperature in terms of °C
$V$	Voltage, $V$
$W$	Power, $W$
$\varepsilon$	Effectiveness (-)
$\omega$	Absolute humidity, $kg (vapor)/kg (dry air)$ .

$\Delta$	difference or change
<b>Subtitle</b>	
a	Air
b	Bottom
br	Brain water
d	Dehumidifier
da	Dry air
dw	Desalinated water
fw	Fresh water
fg	The enthalpy (entropy, etc) required for evaporation, (J/kg)
h	Humidifier
in	input
Max	Maximum
out	output
sw	Seawater, Saline water
t	Top

## REFERENCES

- Abdullah, A., Panchal, H., Alawee, W. H., & Omara, Z. (2023). Methods used to improve solar still performance with generated turbulence for water desalination-detailed review. *Results in Engineering*, 101251. <https://doi.org/10.1016/j.rineng.2023.101251>
- Arabi, M. K. A., & Reddy, K. V. (2003). Performance evaluation of desalination processes based on the humidification/dehumidification cycle with different carrier gases. *Desalination*, 156(1-3), 281-293. [http://dx.doi.org/10.1016/S0011-9164\(03\)00359-X](http://dx.doi.org/10.1016/S0011-9164(03)00359-X)
- Bose, D., Goyal, K., & Bhardwaj, V. (2017). *Design and development of a solar parabolic concentrator and integration with a solar desalination system*. GRIN Verlag. <https://www.grin.com/document/377110>
- Chehayeb, K. M., Narayan, G. P., & Zubair, S. M. (2014). Use of multiple extractions and injections to thermodynamically balance the humidification dehumidification desalination system. *International Journal of Heat and Mass Transfer*, 68, 422-434. <https://doi.org/10.1016/j.ijheatmasstransfer.2013.09.025>
- Dehghani, S., Date, A., & Akbarzadeh, A. (2018). Performance analysis of a heat pump driven humidification-dehumidification desalination system. *Desalination*, 445, 95-104. <https://doi.org/10.1016/j.desal.2018.07.033>
- Dehghani, S., Date, A., & Akbarzadeh, A. (2019). An experimental study of brine recirculation in humidification-dehumidification desalination of seawater. *Case Studies in Thermal Engineering*, 14, 100463. <https://doi.org/10.1016/j.csite.2019.100463>
- Dehghani, S., Mahmoudi, F., & Akbarzadeh, A. (2020). Experimental performance evaluation of humidification-dehumidification system with direct-contact dehumidifier. *Journal of Energy Resources Technology*, 142(1). <https://doi.org/10.1115/1.4044551>
- Easa, A. S., Khalaf-Allah, R. A., Mohamed, S. M., Habba, M. I., & Tolan, M. T. (2024). Optimization of Humidification-Dehumidification solar desalination Unit: Comparative analysis. *Applied Thermal Engineering*, 236, 121610. <https://doi.org/10.1016/j.applthermaleng.2023.121610>
- Elattar, H., Fouda, A., & Nada, S. (2016). Performance investigation of a novel solar hybrid air conditioning and humidification-dehumidification water desalination system. *Desalination*, 382, 28-42. <https://doi.org/10.1016/j.desal.2015.12.023>
- Elhenawy, Y., Bassyouni, M., Fouad, K., Sandid, A. M., Abu-Zeid, M. A. E.-R., & Majazi, T. (2023). Experimental and numerical simulation of solar membrane distillation and humidification-dehumidification water desalination system. *Renewable Energy*, 215, 118915. <http://dx.doi.org/10.3390/membranes13100821>
- Fang, S.-C. (2022). Evaluation of low energy consumption control for seawater desalination on Penghu Island. *Energy & Environment*, 0958305X221127649. <https://doi.org/10.1177/0958305X221127649>
- Garcia-Rodriguez, L. (2002). Seawater desalination driven by renewable energies: a review. *Desalination*, 143(2), 103-113. [https://doi.org/10.1016/S0011-9164\(02\)00232-1](https://doi.org/10.1016/S0011-9164(02)00232-1)
- Hamed, M. H., Kabeel, A., Omara, Z., & Sharshir, S. (2015). Mathematical and experimental investigation of a solar humidification-dehumidification desalination unit. *Desalination*, 358, 9-17. <http://dx.doi.org/10.1016/j.desal.2014.12.005>
- Herez, A., El Hage, H., Lemeland, T., Ramadan, M., & Khaled, M. (2020). Review on photovoltaic/thermal hybrid solar collectors: Classifications, applications and new systems. *Solar Energy*, 207, 1321-1347. <https://doi.org/10.1016/j.solener.2020.07.062>
- Hermosillo, J.-J., Arancibia-Bulnes, C. A., & Estrada, C. A. (2012). Water desalination by air humidification: Mathematical model and experimental study. *Solar Energy*, 86(4), 1070-1076. <https://doi.org/10.1016/j.solener.2011.09.016>
- Hosseini, S., & Sarhaddi, F. (2017). Performance assessment of a humidification-dehumidification desalination unit connected to photovoltaic thermal collectors. *Amirkabir Journal of Mechanical Engineering*, 49(3), 653-662. <https://doi.org/10.22060/mej.2016.765>
- Kadhom, M. (2023). A review on the polyamide thin film composite (TFC) membrane used for desalination: Improvement methods, current alternatives, and challenges. *Chemical Engineering Research and Design*. <https://doi.org/10.1016/j.cherd.2023.02.002>
- Lai, L., Wang, X., Kefayati, G., & Hu, E. (2023). Analysis of a novel solid desiccant evaporative cooling system integrated with a humidification-dehumidification desalination unit. *Desalination*, 550, 116394. <http://dx.doi.org/10.1016/j.desal.2023.116394>
- Lall, U., Heikkila, T., Brown, C., & Siegfried, T. (2008). Water in the 21st century: Defining the elements of global crises and potential solutions. *Journal of International Affairs*, 1-17. <https://www.jstor.org/stable/24358108>
- Luberti, M., & Capocelli, M. (2023). Enhanced Humidification-Dehumidification (HDH) Systems for Sustainable Water Desalination. *Energies*, 16(17), 6352. <https://doi.org/10.3390/en16176352>
- Mortezapour, H., Mostafavi, M. H., Jafari Naeimi, K., & Shamsi, M. (2018). Experimental Analysis of a Humidification-Dehumidification Solar Desalination System Equipped with a Photovoltaic-Thermal Collector. *Iranian Journal of Biosystems Engineering*, 49(2), 295-305. <https://doi.org/10.22059/ijbse.2017.241910.664985>
- Naeni, A., Jalali, A., & Houshfar, E. (2023). Thermodynamic and thermoeconomic modeling of humidification-dehumidification desalination systems with bubble column dehumidifier. *Desalination*, 568, 117005. <https://doi.org/10.22059/ijbse.2017.241910.664985>
- Narayan, G. P., Mistry, K. H., Sharqawy, M. H., Zubair, S. M., & Lienhard, J. H. (2010). Energy effectiveness of simultaneous heat and mass exchange devices. <http://dx.doi.org/10.5098/hmt.v1.2.3001>
- Narayan, G. P., Sharqawy, M. H., Summers, E. K., Lienhard, J. H., Zubair, S. M., & Antar, M. A. (2010). The potential of solar-driven humidification-dehumidification desalination for small-scale decentralized water production. *Renewable and sustainable energy reviews*, 14(4), 1187-1201. <https://doi.org/10.1016/j.rser.2009.11.014>
- Sahay, A., Sethi, V., Tiwari, A., & Pandey, M. (2015). A review of solar photovoltaic panel cooling systems with special reference to Ground coupled central panel cooling system (GC-CPCS). *Renewable and sustainable energy reviews*, 42, 306-312. <https://doi.org/10.1016/j.rser.2014.10.009>
- Srija, M., Bhandari, S., & Prasad, T. (2022). Quaternary Recycling Studies for Desalination Membrane Management. In *Sustainable Chemical, Mineral and Material Processing: Select proceedings of 74th Annual Session of Indian Institute of Chemical Engineers (CHEMCON-2021)* (pp. 121-132). Springer. <https://link.springer.com/book/10.1007/978-981-19-7264-5>
- Srithar, K., & Rajaseenivasan, T. (2017). Performance analysis on a solar bubble column humidification dehumidification desalination system. *Process safety and environmental protection*, 105, 41-50. <https://doi.org/10.1016/j.psep.2016.10.002>
- Xue, T., Yang, F., Zhao, X., He, F., Wang, Z., Wali, Q., Fan, W., & Liu, T. (2023). Portable solar interfacial evaporator based on polyimide nanofiber aerogel for efficient desalination. *Chemical Engineering Journal*, 461, 141909. <https://dx.doi.org/10.2139/ssrn.4289747>
- Zhou, S., Zhang, K., Yang, W., Zhu, X., & Shen, S. (2023). Evaluation of a heat pump coupled two-stage humidification-dehumidification desalination system with waste heat recovery. *Energy Conversion and Management*, 278, 116694. <https://doi.org/10.1016/j.enconman.2023.116694>